ELSEVIER

International Journal of Mass Spectrometry 205 (2001) 209–226

International Journal of Mass Spectrometry

The working principle of the trochoidal electron monochromator revisited

V. Grill, H. Drexel, W. Sailer, M. Lezius, T.D. Märk*,†

Institut für Ionenphysik, Universität Innsbruck, Technikerstrasse 25, A-6020 Innsbruck, Austria

Received 21 July 2000; accepted 28 August 2000

Abstract

On the basis of a number of different experiments employing various principles, we have demonstrated that the energy resolution of the trochoidal electron monochromator used in our laboratory the past 5 yr is not independent from the electron energy used, that is, the very high nominal-energy-resolution close-to-zero electron energy in the range of several meV deteriorates quickly with increasing electron energy reaching values of up to 100 meV at ~1-eV electron energy. Carrying out extensive electron trajectory calculations with the Simion program, we were able to show that our variant of a trochoidal monochromator does not only operate on the trochoidal dispersion principle but also involves a retarding field component right after the dispersion region in achieving this high-energy-resolution close-to-zero energy. This retarding field is, however, weakened at higher electron energies (caused by the influence of the electron-acceleration field) leading to the decrease in energy resolution with increasing electron energy. On the basis of further simulations, we have designed and constructed a new monochromator avoiding this and other deficiencies. This new monochromator currently has an energy resolution of ~45 meV independent of the electron energy. Further improvements are under consideration. (Int J Mass Spectrom 205 (2001) 209–226)

Keywords: Electron monochromator; Trochoidal monochromator; Energy resolution; Electron trajectory simulations

1. Introduction

A detailed understanding of the interaction of electrons with atoms and molecules is an important prerequisite for various research areas in physics, chemistry, biology/medicine, atmospheric physics, material processing, and so forth. In many cases, one basic requirement for studies in these areas is the production of electrons with well-defined properties, especially regarding energy and angular distribution. Electron monochromators are devices that produce such well-defined electron beams. The monochromator type most commonly used is the hemispherical monochromator (HM), which uses hemispherical deflector plates to obtain the desired energy selection. Hemispherical monochromators are mostly used for surface analysis, that is, LEED, Auger, and so forth, and the best resolution achievable with these devices is ~0.9 meV [1]. However, an important drawback of monochromators based solely on electrostatic deflection is that they, in general, need to be operated at electron energies exceeding several eV (usually 2–4 eV is the lower limit). Electrons with lower energies

* Corresponding author. E-mail: tilmann.maerk@uibk.ac.at

† Also adjunct professor at Dept. Plasmaphysics, Comenius University, Bratislava, SK-84215

Dedicated to Professor Aleksandar Stamatovic on the occasion of his 60th birthday.

1387-3806/01/$20.00
PII S1387-3806(00)00378-X

are increasingly sensitive to stray fields and easily get lost from the interaction region. However, the energy range at almost zero eV is particularly interesting for studies in the gas phase. For this low-energy range, a different type of monochromator has been used for several decades [2,3]. In this case, to prevent slow electrons from leaving the interaction region, a guiding axial magnetic field is used in addition to an electrostatic field. Such a magnetic field intrinsically induces a very distinct mode of operation compared to pure electrostatic deflection. It is the purpose of this article to discuss and elucidate the advantages and disadvantages of such a device, which is generally referred to as trochoidal monochromator (TM) [3].

The original TM, first built by Barr and Perkins [2], was used as an energy analyzer for electrons produced in a plasma. These authors used an $E \perp B$ (E field and B field crossed at right angles) field to disperse electrons according to their velocity in the crossed-field region. It is important to note that such an energy selection is only sensitive for the velocity component in a forward direction. Therefore, for an optimal application of the TM principle, it would be desirable to convert the velocity components of the electrons to be analyzed into a forward direction if the original angular distribution of the electrons is not uniform. This conversion can be achieved by using the adiabatic invariance of the magnetic field, that is, changing from a region of high magnetic field strength in the production region of the electrons to be analyzed to a comparably low magnetic field in the $E \perp B$ analyzer. This technique has been applied with advantage by Barr and Perkins [2], using a magnetic field of 23 kG in the production region (i.e., the plasma) and of 1.2 kG in the region of the $E \perp B$ field.

The first successful attempt to apply the equivalent principle for an energy selective electron source was carried out by Stamatovic and Schulz [3,4]. Using one fixed magnetic field of ~50 G, they reported an energy resolution of ~20 meV down to almost 0 eV. Since this first realization of such an electron source, the trochoidal monochromator has found a widespread application; most interestingly, the resolution achieved and reported was seldom better than ~75 meV. Because of the increasing interest in trochoidal monochromators, a number of articles explored the principle of operation of trochoidal monochromators [2,4–6]. These fundamental theoretical studies will be summarized in section 3 of this article. In several articles, important methods to improve the performance of the TM device have been suggested regarding both electron current and resolution. For a comparison of the many different TM instruments reported in the literature, the best resolution achieved (the one normally stated in the papers) will be used here. Nevertheless, an intrinsic problem connected to the energy resolution claimed in a specific study is the method of its determination. The method most commonly applied is to employ a calibration gas with a known cross-section shape (for details, see ref. [7]). Best suited for such a purpose is a molecule that shows s-wave attachment at very low electron energies leading to the formation of a long-lived negatively charged parent ion (as is the case for SF_6^-) or via dissociative electron attachment (DEA) to the formation of a stable fragment ion (as, for instance, Cl^- from CCl_4). S-wave cross sections are generally huge, and their shape can be interpreted as a delta function. Then, the full-width-half-maximum (FWHM) of the negative ion signal measured around zero energy corresponds approximately, that is, within the accuracy of the measurement, to the energy resolution of the electron beam itself (without need of further deconvolution). We will discuss important drawbacks of this method (see, also, ref. [7]) and of several other ways used to determine energy resolutions below (section 2).

In addition, electron trajectory simulations for different trochoidal monochromator geometries will be presented here (see section 4). A new electron optical design, created after detailed studies of the theoretical papers together with the results obtained by the simulations, will be discussed in the last section. The first experimental results obtained using this new design will also be presented in this final section.

2. Determination of the energy resolution

The quality of its electron energy distribution characterizes an electron monochromator. As already

mentioned, the determination of the resolution is, in most cases, done using a calibration gas with a large s-wave attachment cross section around zero electron energy. This method is easy to employ, and it provides the determination of the zero-energy point of the energy scale. Moreover, using such a technique it is not necessary to incorporate an additional device for measuring the energy resolution directly, as with a retarding field analyzer. However, it must always be remembered that this is only an indirect method and that it can lead to a severe misjudgment of the performance of the device. We will demonstrate here that the FWHM of the negative ion signal of an s-wave attachment process is not necessarily a measure of the resolution of the monochromator, at least regarding the trochoidal monochromator in use in Innsbruck [8]. This monochromator was constructed following the design described in the original paper by Stamatovic and Schulz [3].

One possible candidate to determine the energy resolution by using a negative ion signal is tetrachlormethane, CCl_4. The cross section for the formation of Cl^-/CCl_4 by electron attachment shows a very pronounced peak at zero electron energy that is typical for most s-wave attachment processes. The CCl_4 molecule is especially suited as a test molecule because several groups have studied its attachment cross section in great detail [7–14]. One of the most advanced studies has been performed by Hotop and coworkers [9], using laser photoelectrons to measure the attachment cross section from sub-meV to ~160 meV with an energy resolution <1 meV (see Fig. 1). With such high-resolution data, the authors could confirm the threshold dependence for s-wave attachment predicted by theory [15], which predicted an E^{-1} dependence for electron energies larger than ~10 meV and an $E^{-1/2}$ dependence for lower energies. In addition, Hotop and coworkers reported the observation of a coupling between the dissociative attachment channel and the symmetrical stretch vibration leading to two downward cusps in the attachment function at $E(v_1) = 56.9$ meV and $E(2v_1)$ [9]. On the basis of such data, we decided to use CCl_4 as a calibration gas in this study (see, also, our earlier investigations with this gas [7]). In Fig. 2, a typical Cl^- signal produced after electron attachment to CCl_4 as a function of electron acceleration voltage in our (up to very recently used) trochoidal monochromator (see Fig. 3) is shown. The FWHM derived in this case is 12 meV. However, a comparison, in Fig. 1, of our results with the high-resolution data published by Hotop et al. [9], that is, after convoluting their data with a Gaussian curve of 12 meV FWHM, immediately shows that although the two steps get washed out slightly by the convolution, it should still be possible to observe some structure in our experiment. As we do not observe any structure at these energies $E(v_1)$ and $E(2v_2)$, we had to conclude that the measured FWHM in our experiment does not fully describe the overall energy resolution or that the structures reported by Hotop and coworkers [9] have a different origin because of the laser photoelectron attachment technique used.

We want to note here that, depending on the exact shape of the cross section at very low electron energies, the FWHM of the convoluted curve will slightly differ from the FWHM of the Gaussian one. This has to be taken into account when trying to compare convoluted curves exactly with measured data. In the case here, we only wanted to give an estimate of the resolution necessary to observe the fine structures.

To exclude any particularities related to CCl_4, we repeated the same experiment for electron attachment to methyliodide, which leads to the production of I^- at zero energy. In this case, Hotop and coworkers have reported a similar, most remarkable structure at ~700 meV [16]. But also in this case, we were not able to observe any structure besides the usual sharp zero-energy resonance present in our experiment. A possible explanation for our inability to reproduce structures several 10 meV above nominal zero eV, even if the FWHM at zero energy is sufficiently small, would be that the FWHM at zero energy does not represent the electron energy resolution for all electron energies. To prove such a hypothesis, we need to employ a different, independent measure of the energy resolution. In a first attempt, we used a simple retarding field method by measuring the electron current with a picoamperemeter at the electron col-

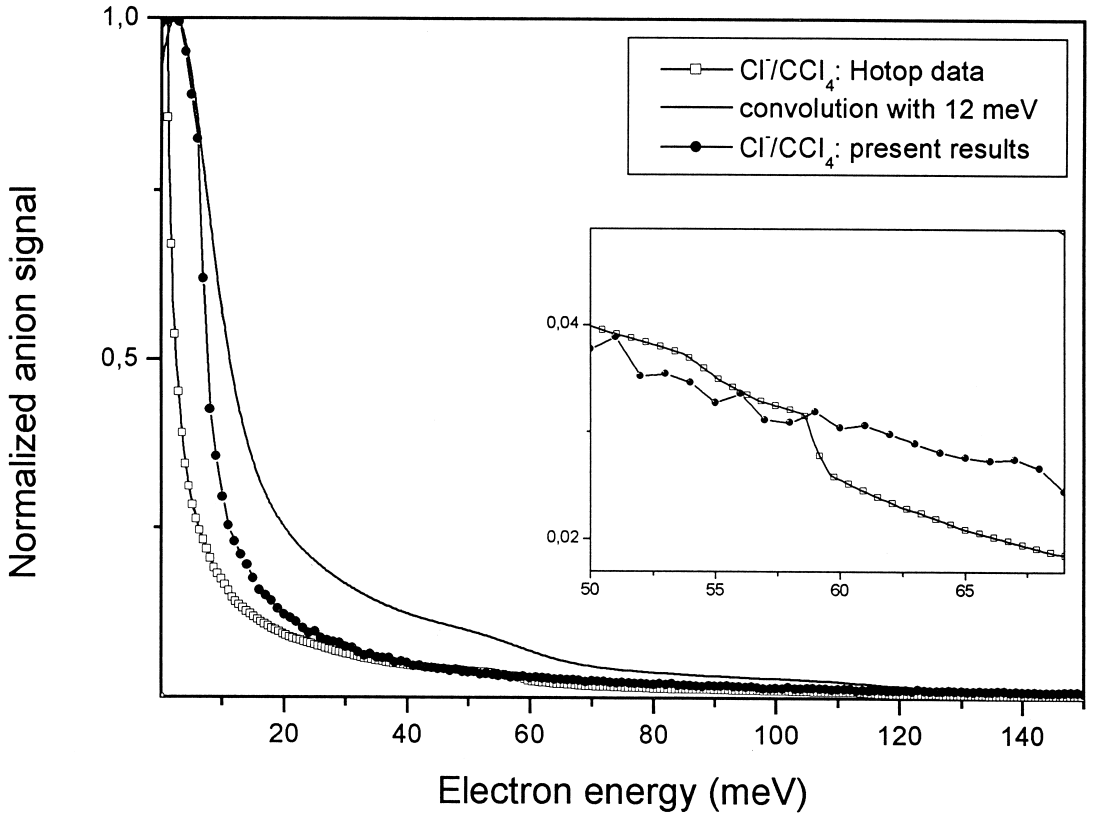

Fig. 1. Dissociative electron attachment to CCl_4, measured by Hotop and coworkers [9] (the original data have been generously provided by these authors) with laser photoelectrons (open squares) and in this lab with free electrons (filled circles). The convolution of the data of Hotop and coworkers [9] with a 12-meV Gauss curve is also shown to allow a meaningful comparison with the data from this lab (solid line). The enlarged region shows the 55-meV cusp in the Hotop et al. data [9], as compared to the present results.

lector as a function of a retarding voltage with respect to the collision chamber. The retarding potential curve measured simultaneously with the Cl^- signal shown in Fig. 2 is displayed together with the differentiated signal. The FWHM of the differentiated electron current, which is a measure of the energy resolution, is ~37 meV and, hence, three times larger than the FWHM of the Cl^- curve. On the basis of this large discrepancy, we decided to introduce a more sophisticated retarding field analyzer after the collision chamber, which will be discussed in a later section.

As a further test concerning our energy resolution over a somewhat larger energy range, we attempted to reproduce data published by Stamatovic and Schulz [17] for a scavenging process involving electron attachment to SF_6 in an SF_6/CO_2 mixture. In such an experiment, the electrons become inelastically scattered at the CO_2 molecules, thereby losing energy in quanta of CO_2 vibrational excitations. Consequently, in the case when the original energy of the electrons coincides with the vibrational excitation energy of the CO_2 molecule, attachment to SF_6 is enhanced. This experiment is especially suitable to check the energy resolution at somewhat higher electron energies; in the energy range from zero to 300 meV, four distinct peaks are reported that can be clearly resolved with an electron energy resolution of 50 meV. Because of the lower pressure used in our experiment, the overall amount of scavenging was smaller than that reported by Stamatovic and Schulz [17], but it was definitely present in our experimental runs. Nevertheless, it was not possible to resolve the single scavenging peaks

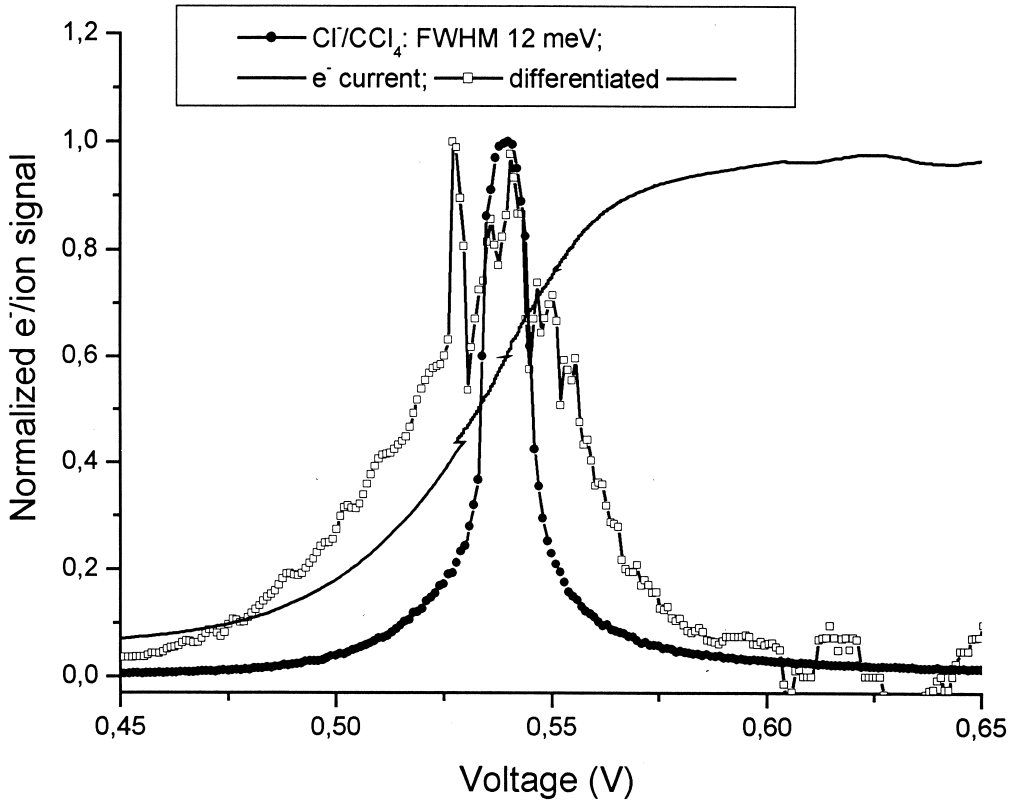

Fig. 2. Cl^- signal after dissociative electron attachment to CCl_4 as a function of electron acceleration voltage (filled circles). The FWHM of this anion peak is 12 meV. The electron current measured under the same conditions is shown in the same graph as a function of the retarding potential (solid line). The first derivative of the electron current curve (open squares) shows a FWHM considerably larger than the width of the Cl^- curve. Note that the data points (circles, squares) are connected by a line to guide the eye.

although the resolution, as deduced from the FWHM of the zero energy peak, was always <50 meV.

If nothing else, these various experimental results indicated to us that the energy resolution does not remain constant during variation of the electron energy in our experiment. To confirm the loss in resolution for higher electron energies, a further test was performed, that is, measuring the onset for the production of O^- from NO at ~7.5 eV. The production of this anion is especially appropriate for testing the energy resolution at higher electron energies because the production channel $O^-(^2P) + N^*(^2D)$ shows a sharp onset at ~7.5 eV [18–20]. In Fig. 4, the energy resolution at ~7 eV electron energy (as determined by taking the FWHM of the differentiated O^- curve) is compared with the energy resolution at

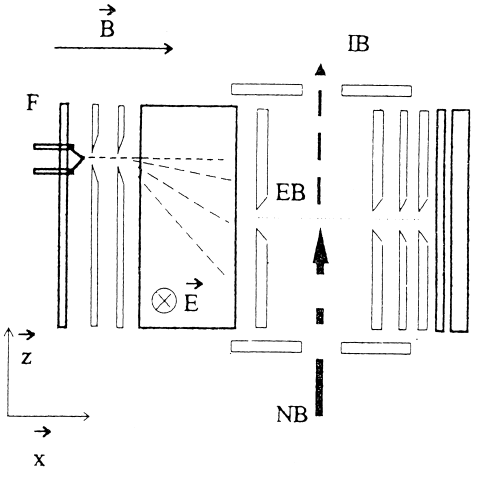

Fig. 3. Schematic view of the trochoidal monochromator used until very recently in our lab. Adapted from [7].

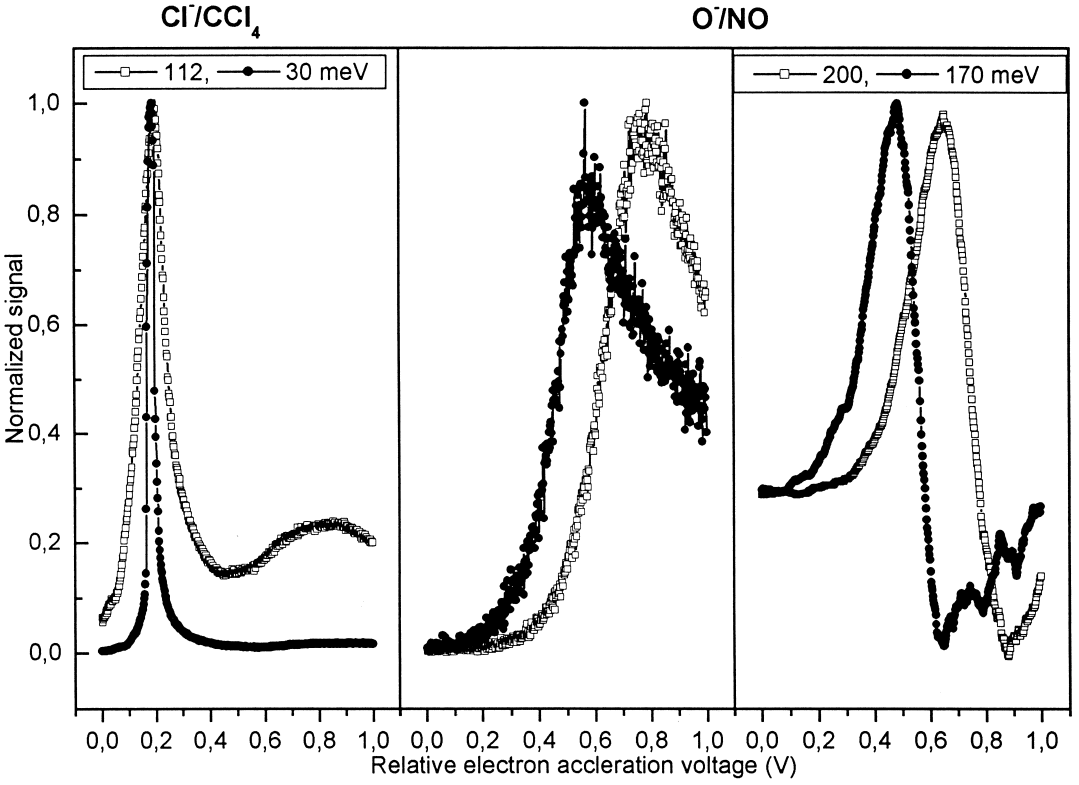

Fig. 4. Dissociative electron attachment to a NO/CCl_4 mixture comparing the energy resolution at almost zero electron energy (with s-wave attachment to Cl^-/CCl_4) and at 7.5 eV (with the appearance energy for O^-/NO). In the left panel, the zero-energy resonance for Cl^-/CCl_4 is shown for two different energy resolution, that is, 30 meV (filled circles) and 112 meV (open squares). The center panel shows the appearance energy curves for the production of O^-/NO at ~7.5 eV measured under the same experimental conditions as the energy resolutions for Cl^-/CCl_4. To determine the energy resolution, these curves have been smoothed and differentiated, as shown in the right panel. The FWHMs obtained are a measure of the energy resolution at ~7.5 eV and are 170 and 200 meV, respectively. The curves with equal lens settings have corresponding symbols in all three panels. One has to note that the energy scale is not corrected and that the different data sets have been shifted for the sake of clarity.

zero eV (as determined by the FWHM of the Cl^- curve) for different settings of the zero-energy resolution. As can be seen, the loss in resolution is more pronounced in the case of a very narrow Cl^- peak at zero energy, that is, in the case of a 30-meV FWHM Cl^- peak, the O^-/NO curve shows a 170-meV FWHM, whereas for a 112-meV Cl^- peak, the O^-/NO curve yields a FWHM of 200 meV.

In the course of these various tests on the operation of the TM, we observed another interesting feature. In most cases, when tuning the TM to achieve a good performance using the zero-energy resonance of Cl^- from CCl_4, we saw a double peak structure with a small distribution sitting on top of a very broad foot. Hence, we had to conclude that in our experiment at least two electron distributions are present at the same time. The second distribution may be caused by electrons reflected twice from the surfaces of the dispersive element, a phenomenon that has been mentioned by Allen [21]. Importantly, in many cases, it is not possible to tell if in our experiment the observed resonance results from one or two distributions. A perfect overlap of the two distributions can easily simulate the presence of a single distribution.

As a result of these experiments, one can in the best case conclude that the resolution of the electron energy is not constant with electron energy but, rather, deteriorates very quickly above threshold. We will see

below that one possible reason for a severe loss of resolution lies in the influence of the changing electron acceleration voltage when scanning the electron energy. A second cause may lie in the difficulties in producing true zero-energy electrons themselves. If in the collision region only small stray potentials are present (e.g., caused by contact potentials), the electrons would have to cross a potential barrier before interacting with the molecular beam. In such a case, it is impossible to have zero-energy electrons interacting with the gas, and thus, the negative ion signal would both be cut toward low energies and present only part of the real cross section.

Unfortunately, none of the previously published theories of the trochoidal operation principle could explain the behavior of our monochromator, as described above, satisfactorily. Therefore, we decided to perform electron trajectory simulations using the three-dimensional lens-geometry optimization program Simion [22]. The main goal of these simulations was to clarify the discrepancy in our measurements with the theoretical predicted performance and to understand the influence of the different lenses on the theoretical resolution of the electron energy. In addition, our aim was to find ways to improve the performance of the trochoidal monochromator by successive changes in the electron optical design. However, before presenting the results of these simulations, it is appropriate for a better understanding of the operation principle to review the theoretical studies concerning trochoidal monochromators.

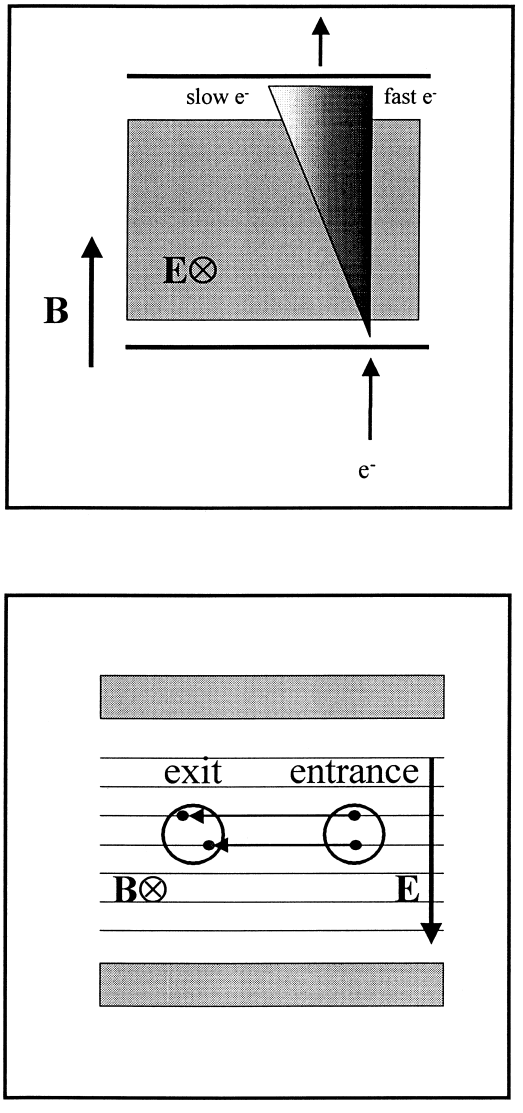

Fig. 5. Schematic view of the $E \perp B$ region in the dispersive element. In the upper panel the deflection of the electrons as a function of their velocity in forward direction is shown, that is, the slower electrons are deflected more strongly. In the lower panel, the influence of the voltage drop across the entrance electrode is shown, that is, the electrons entering at the upper edge of the orifice are deflected more strongly than those entering at the lower edge because of the deceleration effect at the upper part of the electrode.

3. Theory: operating principle

A description of the operating principle of a trochoidal monochromator, which incorporates a $E \perp B$ field with the B field directed along to the electron path, can be found in almost every textbook on general physics (see, also, Fig. 5). In short, following the description given in reference [2], the time the electron spends in the E field of length L can be expressed as

$$t = \frac{L}{v_{II}}, \tag{1}$$

where v_{II} is the velocity component parallel to the magnetic field lines. The distance, X, the electron will drift during this time follows as

$$X = v_d t, \tag{2}$$

with

$$\vec{v}_d = \frac{\vec{E} \times \vec{B}}{B^2}. \quad (3)$$

Hence, the displacement X can be expressed as

$$X = \frac{EL}{Bv_{II}} \quad (4)$$

and gives the displacement as a function of the parallel component of the velocity. Converting this to the parallel component of the kinetic energy W_{II}, which is the energy the electrons must have to exit the crossed field region with the necessary displacement X, gives

$$W_{II} = \frac{1}{2} m_e \left(\frac{EL}{BX}\right)^2. \quad (5)$$

From these equations, it is easy to understand that the displacement in the crossed field is only sensitive to the parallel component of the energy. The perpendicular energy $W_\perp$, however, becomes only important if this component is so large that the orbital diameters of the electrons become comparable to the size of any of the lens orifices. This can be the case when electrons are emitted from the filament under high emission angles leading to large gyration radii. Such large $W_\perp$ would increase the width of the transmitted electron energy of the analyzer significantly [2].

Regarding the energy resolution of such a device, Barr and Perkins [2] gave the transmission through the crossed field region as a function of the kinetic energy W_{II}. They found that the energy resolution deteriorated rapidly for Δ/X_0 larger than ~0.2, especially on the high-energy side, with Δ/X_0 being the ratio of slit width Δ to slit displacement X_0. Stamatovic and Schulz [4] deduced an expression for the energy resolution that has been used as the starting assumption for several other papers. These authors gave the energy spread Δw as a function of the electric field E, the magnetic field B, the displacement D, the sum of the entrance and exit aperture ΔD, the length of the crossed field L, the mass and charge of the electron m_e and e, and the entrance slit diameter S_1:

$$\Delta w = \frac{E^2 L^2 \cdot m_e \Delta D}{B^2 D^3} + eES_1. \quad (6)$$

This equation gives the maximum energy spread (later called base value), which amounts to two times the experimentally determined FWHM. The first term in this equation is related to the dispersive principle, while the second term is caused by the voltage drop across the entrance or exit electrode (whichever is smaller). The derivation of Eq. (6) is actually based on several assumptions, such as, negligible space charge, that is, the individual electron orbits; uniform electric field in the crossed field region, that is, the boundary effects can be neglected; and $v_\perp$ is negligible for each electron, that is, there is no gyration of the incident electron beam.

The voltage drop in the second term, which has been discussed in more detail by several authors [23,24], is often the resolution-determining part [5]. To understand the origin of this term, one has to visualize the dispersive element not in the direction of the beam deflection but perpendicular to it (see Fig. 5, lower panel). The electrons passing through the entrance electrode at different positions will experience different electric field lines and, depending on their entrance position in y direction (this is the direction parallel to the electric field), they will get either decelerated or accelerated. This change in velocity at the entrance electrode will consequently change the deflection in the crossed field. Hence, these electrons will exit at a slightly different position in x direction depending on their different positions in the entrance electrode. At the exit electrode, the same effect can be observed and the energy of the electrons will be modified in a similar way. Hence, if the aperture sizes are similar, the velocity will be changed back to the original value, but the resolution-deteriorating effect has already taken place. From this it can easily be understood that in Eq. (6) the diameter of the smaller electrode has to be taken to calculate the resolution of the device.

A more detailed discussion of the influence of this voltage drop and the necessity to include this second term has been given in two slightly different ways. McMillan and Moore [24] have described this effect as being due to a shearing of the original circular cross section of the electron beam into a tilted shape, with the shear angle θ being a function of magnetic field,

electric field, length of the crossed field region, and displacement of the entrance and exit electrode:

$$\tan\theta = \frac{e}{m_e} \times \frac{D^3 B^2}{EL^2}. \quad (7)$$

These authors, hence, suggested the use of a tilted slit as the exit electrode to improve both resolution and transmission. The analogous problem of different drift times in the dispersive element because of acceleration/deceleration at the voltage drop of the entrance electrode has been treated by Romanyuk and coworkers [6] in a novel way. Instead of using the tilted slit [24], the authors introduced a nonuniform electric field to compensate for the time differences with a change in the drift velocity. Similarly, Williams and O'Neill [23] have described the influence of the voltage drop at the entrance electrode in terms of an energy transformation, as opposed to a spatial one. These authors found that the additional term for the energy spread at a given position y (with y parallel to E) is independent of the electric field E and only determined by the geometry of the monochromator.

$$\Delta w(y) = 2eEy + \frac{4w_0}{D} \cdot [\sqrt{R_1^2 - y^2} + \sqrt{R_2^2 - y^2}] \quad (8)$$

gives the full energy spread of the beam caused by the voltage drop across the electrodes, with R_1 and R_2 the radii of the entrance and exit apertures and w_0 the total energy of the electrons. For $y = 0$, this equation reduces to the original equation of Stamatovic and Schulz [4]:

$$\frac{\Delta w}{w_0} = \frac{2\Delta D}{D}, \quad (9)$$

from which Eq. (6) has been deduced. For sufficiently high pass energies, the resolution of the instrument will converge to the geometrical limit of the instrument, as given for $y = 0$ [23]. In this case, the potential drop across the aperture ceases to be of major importance.

The most extensive theoretical discussion of trochoidal monochromators has been given by Roy [5], including detailed calculation on the FWHM and the electron transmission for different geometries, electric, and magnetic fields. But unfortunately, all of these parameters depend on each other, therefore, it is very difficult to arrive at definitive conclusions. The difficulty in stating conclusively which parameter is the most important resolution-determining factor has also been encountered by other authors [23,24]. As an example, we will discuss the dependence of the energy resolution on the deflection voltage: Roy's simulations have shown that the deflection voltage should be as small as possible, with an almost quadratic dependence of the energy resolution on the deflection voltage [5]. The same dependence follows also from Eq. (6). Nevertheless, a decrease of E requires a simultaneous decrease of B [23] if the geometry is to be kept similar. But this leads to a loss in electron beam confinement and, consequently, to a loss of resolution and transmission [24].

In addition to this complicated nature of various cross dependences, certain quantitative aspects of the simple monochromator action have yet to be considered in detail [23]. To get a more detailed understanding of the operating principle, electron trajectory studies for different geometries have been performed and will be discussed below.

4. Electron trajectory simulation

According to the theory [4] (see Eq. [6]), the resolution of the trochoidal monochromator in Innsbruck should be ~170 meV (base value), that is, resulting in a FWHM of ~85 meV (with a magnetic field of 25 G and 0.2 V deflection voltage). This value is definitely much worse than the actual FWHM deduced for zero energy, which is in the order of only 5 meV [7]. Therefore, electron trajectory studies were carried out to explain this discrepancy. We studied in detail the geometry of the TM we used until very recently [7,8,20,25–30] (Fig. 3; called, in the following, old geometry) and compared it with the geometry of the original TM reported by Stamatovic and Schulz [4]. After understanding some of the possible pitfalls in the various geometries, several other geometries were simulated to optimize the performance of our monochromator. This optimization procedure was carried out in parallel with the construction of a new monochromator, which now behaves much closer to the theory predictions than does our old geometry design TM.

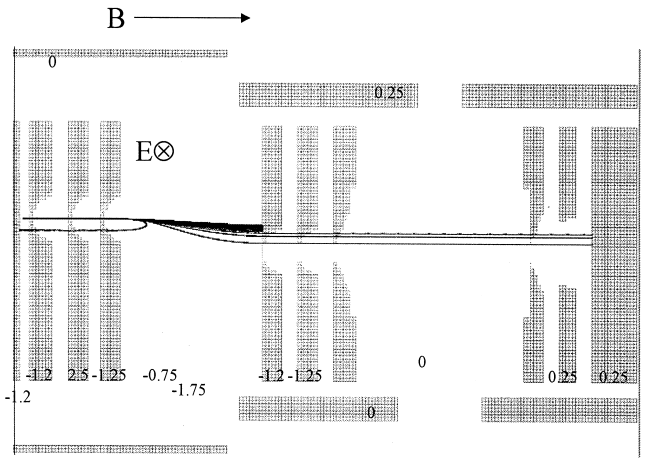

Fig. 6. Cut of the center part of a 3-dimensional Simion simulation of the old geometry (corresponding to the monochromator shown in Fig. 3). The voltages applied to the different electrodes (in V) are included in the figure; the magnetic field was 50 G. The 20 electrons in this simulation all start exactly at the same point but differ in their initial energy. The slowest one starts with 0.08 eV with a subsequent increment of 5 meV. It does not have enough energy to pass the dispersive element, and its trajectory amounts to the maximum deflection angle possible under the present lens settings (which involves a situation with no electron acceleration voltage applied). Nevertheless, the dispersion across the exit orifice is insufficient to achieve high resolution.

4.1. Old geometry

In Fig. 3, the Innsbruck monochromator in its old geometry version is shown. For a better understanding, we show in our simulations a cut at the centerline (e.g., see Fig. 6). Simulating the electron path through the instrument with several different lens settings (all of them were similar to real lens settings during experiments) revealed the true operating principle of this monochromator. Apparently, the geometry of this monochromator is far from perfect, that is, the lens apertures are huge and it is not possible to operate this instrument solely as a trochoidal monochromator to achieve its apparent high resolution. Cutting at both the high- and the low-energy part of the electron distribution with the exit aperture after the deflection element cannot be achieved (see Fig. 6), in particular when simulating electrons starting from the filament under different emission angles and from slightly different spots (see Fig. 7). The best resolution observable in the simulations was worse than 200 meV. Instead, to achieve a high-energy resolution, the lenses after the deflection element must be used to produce a retarding field (see, also, Fig. 8) to cut the low-energy part of the electron distribution. The trochoidal principle is at least partly retained because the high-energy electrons are prevented (see Figs. 6–8) from leaving the deflection element, as these electrons are not deflected far enough to exit through the orifice. It is important to note when using the retarding field at the exit of the dispersive element that the actual exit lens orifice can be smaller than the real one. In such a way, it is possible, in principle, to achieve resolutions better than those given by the equation quoted in the original paper [4] by reducing the second term in Eq. (6). This phenomenon of virtual lens orifices will be discussed in more detail elsewhere [31].

In principle, the usage of such a retarding field can significantly improve the operation of the monochromator, but unfortunately, it involves also a serious drawback. To vary the electron energy, an acceleration voltage has to be applied between the lenses of the monochromator where the electrons are produced and monochromatized and the collision chamber. Unfortunately, because of the missing ion optical shielding between the deflection element and the collision chamber in this geometry, this acceleration voltage severely influences the electron optics in this region. As can be seen in Fig. 8, a change of the acceleration voltage from 100 to 700 mV destroys the retarding potential necessary for high-energy resolution. It is evident that, in such a

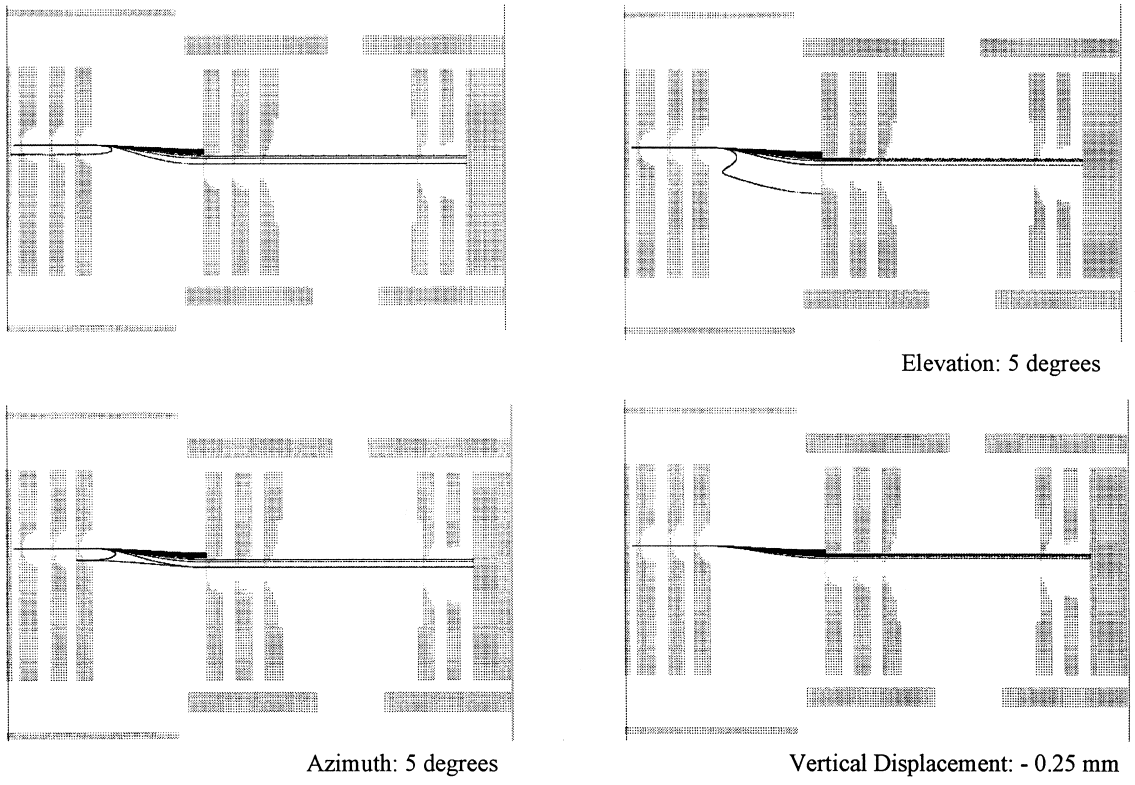

Fig. 7. Cut of the center part of 3-dimensional Simion simulations with the same electrode settings as in Fig. 6. The energy of the electrons is also the same, though the starting conditions, that is, emission angle and emission spot from the filament, are varied. The upper-left panel is only shown for comparison, as all electrons start from the center of the filament, as in Fig. 6. In the upper-right and lower-left panels, the elevation and azimuth angles for all electrons are raised from 0° to 5°, respectively. In the lower-right panel, the electrons start 0.25 mm below the center point.

situation, it is impossible to maintain the same resolution at different energies. Unfortunately, the loss of the retarding field is a decisive factor, leading to a complete loss of resolution immediately above threshold. This fact explains the experimental observation of a narrow anion peak at zero electron energy while being unable to resolve any fine structure above 50 meV (see section 2).

Another drawback of the present geometry is apparent from the electron trajectories shown in Figs. 6 and 7. Because of the velocity-dependent deflection of the electrons in the dispersive element, the spacing between adjacent trajectories (differing by the same amount in energy) is much narrower for fast electrons. Therefore, most electrons leave the dispersive element at the upper edge of the exit orifice because the retarding field rejects the slower electrons, which would, in principle, exit at the lower edge. All electrons are guided by the magnetic field, and they will stay on their magnetic field line. Consequently, all the electrons will pass the following lens orifices and the entrance of the collision chamber at the upper edge of the orifices. Close to the edges of these apertures, inhomogeneous fields are present that can either deflect the electrons according to their energy or even alter their energy. Moreover, in such a situation, any surface charge will influence the electron beam significantly. It is clear that such a lens geometry should be avoided in an improved construction of an electron monochromator. In a more convenient geometry, all the lens orifices following the exit lens have much larger diameters, hence allowing the electrons to pass close to the center, where the electrostatic field is homogenous and the distance to any disturbing surface is large.

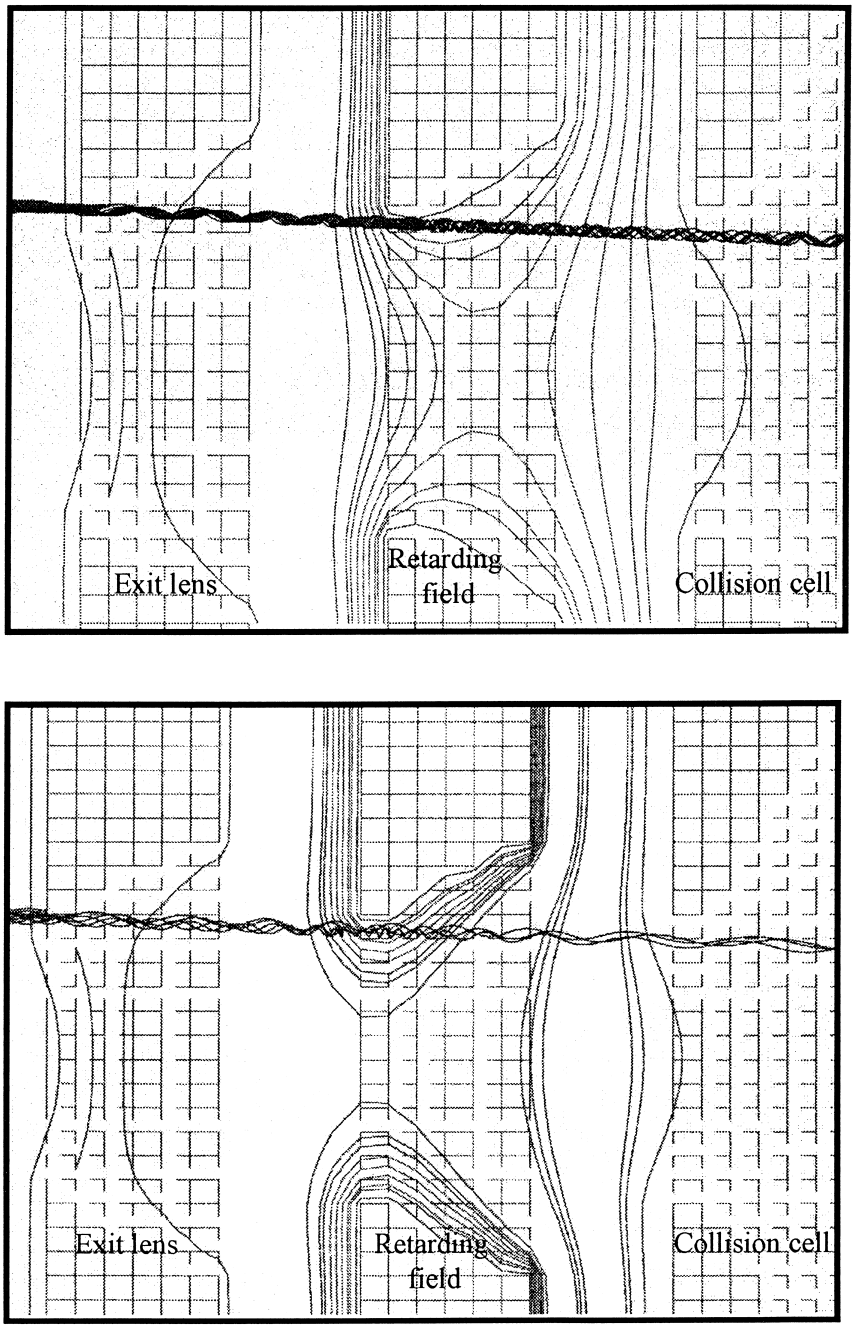

Fig. 8. Influence of the electron acceleration field on the retarding potential in the old geometry. In the upper panel, the potential lines for an electron acceleration voltage of 100 mV is shown, while in the lower panel the electron acceleration voltage is 700 mV. In this simulation, the magnetic field is set at a slight angle with respect to the monochromator axis and the electrons (here only electrons passing close to the upper edge of the exit lens are considered and, thus, this part of the retarding potential is of relevance for the fate of the electrons beyond the retarding field electrode) start from the filament under an emission angle of 10°.

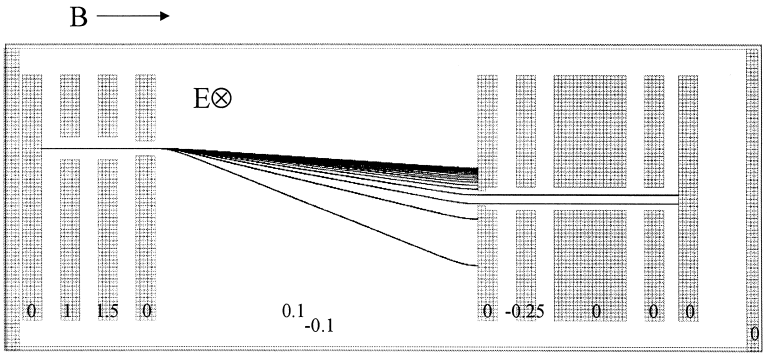

Fig. 9. A cut of the center part of a 3-dimensional Simion simulation for the original TM as published by Stamatovic and Schulz [4] is shown. The voltages applied to the different electrodes (in V) are included in the figure; the magnetic field is 100 G. The electrons have an initial energy of 0.001 eV, increased stepwise by 1 meV.

4.2. Original geometry

To obtain a deeper insight into the working principle of trochoidal monochromators, especially concerning different geometries, and to check if the observed problems are a particular feature of the old TM in Innsbruck, we have also studied the monochromator that was published in the original work of Stamatovic and Schulz [3,4]. It is already evident from Eq. (6) that this original monochromator should give a much higher energy resolution because of the better geometry. The deflection element of the original instrument was 19 mm long (but also 12.7- and 6.3-mm lengths were used) as compared to 6.3 mm in this case, the displacement was 3.2 mm, as compared to 2 mm, and most of the lens orifices were smaller in diameter. A theoretical resolution of 16.5 meV (base value) or ∼8 meV FWHM can be calculated with Eq. (6), using the shortest deflection pair of 6.3 mm and 0.1 V deflection voltage. This value has to be compared to a resolution of 170 meV (base value) or 85 meV FWHM for the present old geometry instrument.

The much better resolution of the original geometry could be also confirmed by Simion simulations, as shown in Fig. 9. Simulations carried out for the experimental parameters given above yield in agreement with the theoretical value of 16.5 meV a resolution of ∼20 meV (base value) using the trochoidal principle, that is, cutting both the high- and low-energy electrons at the exit lens after the dispersive element. It should be noted that by varying these experimental parameters, for instance, increasing the deflection field voltage from 0.1 to 0.2 eV, these simulations yield resolutions in the meV range. Nevertheless, under real experimental conditions, the electrons will not start under the ideal conditions, as assumed for the simulations in Fig. 9. Therefore, the real resolution will be worse. However, this can be ameliorated in practice by operating this TEM, also involving a kind of retarding field potential. Fortunately, the original geometry prevented an influence of the electron acceleration voltage onto the retarding potential, hence preserving the electron distribution while scanning the electron energy. This shielding is achieved by an additional lens, which had been incorporated between the dispersive element and collision region [4]. This extra lens, which has been omitted in most trochoidal monochromators constructed later, was not explicitly discussed in the original paper (or any paper afterwards). Our present Simion simulations demonstrated the proper working of this monochromator as published in the original paper, although the real working principle, that is, the use of an additional retarding potential after the dispersive element, was not discussed. However, Stamatovic and Schulz mentioned in their original paper that they used such a retarding field. Our Simion simulations showed that, although the velocity of the electrons in the dispersive element should be chosen as small as possible to achieve optimum performance, the whole set-up becomes extremely sensitive when a strong retarding field is incorporated in the dispersive element. In addi-

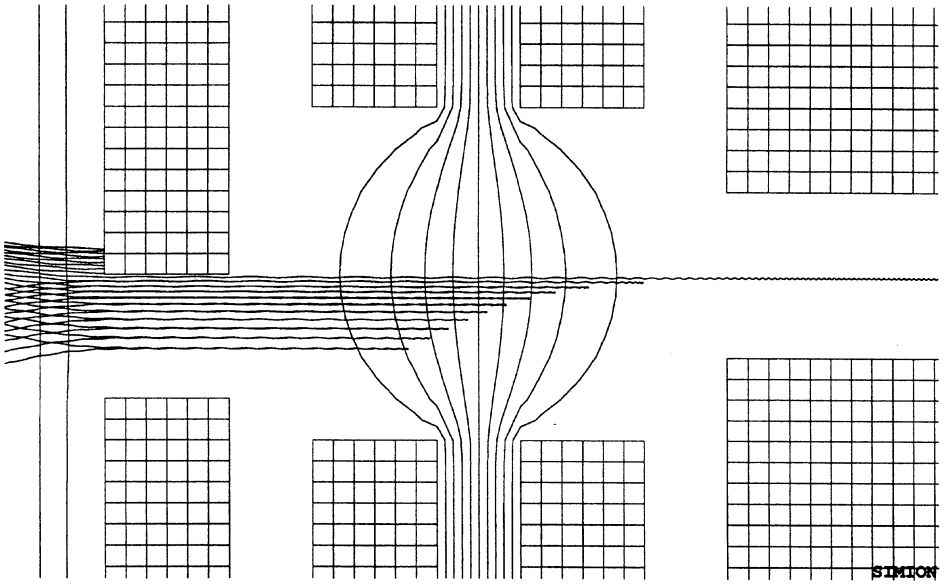

Fig. 10. Simion simulation of the retarding field after the dispersive element.

tion, as can be seen from Eq. (6), the leading term in this equation depends on the voltage drop across the exit or entrance electrode of the dispersive element. By applying a retarding field after the dispersive element, this lens orifice can be made virtually smaller, thus improving the resolution considerably while keeping the whole monochromator in an easy-to-operate mode of operation.

5. Improved monochromator design

On the basis of these results on the working principle of the two monochromators discussed above, we tried to optimize step by step the geometry of our old monochromator. The most important improvements will be discussed in this section. These first changes were all aimed toward a more reliable mode of operation but not primarily toward achieving higher resolution. As a first goal, we were mainly interested in constructing a monochromator capable of an energy resolution that can be easily measured and that is constant over the range of electron energies used. However, we plan in the near future to further optimize the geometry of our monochromator in such a way as to also increase the resolution.

The first important improvement concerns the exit lens of the dispersive element. We decreased its orifice diameter from 1 to 0.4 mm and increased the displacement of the hole to place the upper edge of the orifice onto the centerline of the original lens. This ensured that the electrons cross the subsequent lenses at their center. To be on the safe side concerning surface effects, we increased the diameters of all subsequent lens orifices to 2 mm, including the entrance and exit orifice into the collision region. The simulations showed that the use of such large lens orifices is necessary not only to minimize surface effects but also to ensure proper working in all regions of the monochromator. The electrons should cross all applied fields at a place where the field lines are homogeneously spaced, which usually will be in the center of the lens producing the field (see Fig. 10). It is important to note that such large lens orifices necessitate the use of thick lenses. Otherwise, field penetrations from neighboring lenses can easily distort the center potential. The use of thick lenses has another important advantage: They can be designed to perfectly shield the region before and after the lens involved. This is particularly necessary in the trochoidal monochromator where the retarding field must be shielded from the acceleration field and also in the

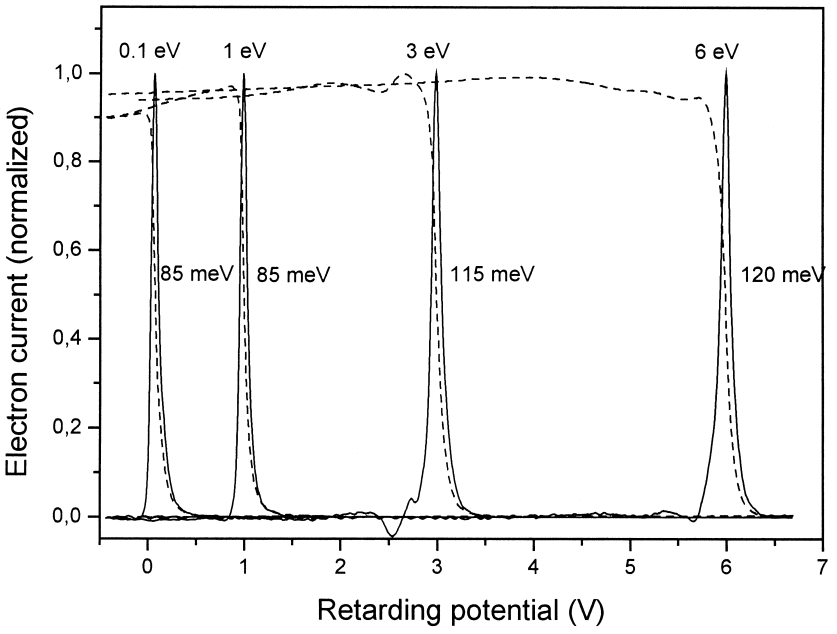

Fig. 11. Electron current versus retarding field for different electron energies (from 0.1 to 6 eV). Note that the alignment of the magnetic field is very crucial as, otherwise, the transmitted electron current varies significantly with energy. The alignment in the present case is still not perfect, as the coils used to generate the magnetic field have not Helmholtz geometry. Hence, the electron current shows some small variations with energy. In addition, the energy resolution of the monochromator, as determined by calculating the FWHM of the differentiated electron current, seems to deteriorate slightly at higher electron energies, that is, in this experimental run from ∼85 meV FWHM at 0.1 eV to ∼120 meV FWHM at 6 eV.

electron ion interaction region. Another advantage of thick lenses is that, otherwise, the well-known effect of energy-dependent transmission through a lens orifice in the presence of an axial magnetic field [32] would modulate the negative ion signal in a more or less unpredictable way. This effect has also been observed in thick lenses if the magnetic field is not perfectly aligned with the centerline of the lens. Instead, we find that with thick lenses and a well-aligned magnetic field, the transmission of the electrons is nearly independent of energy (see Fig. 11).

In Fig. 12, a scaled drawing of the new geometry is shown. We will focus here on the lenses after the dispersive element, as the other lenses have not been changed in their functionality (although slight changes have been carried out). All the lenses after the exit lens of the dispersive element are thicker than 5 mm to ensure a decoupling of the different regions of the monochromator. Before the collision cell there are two regions: the retarding field between exit lens and the first long transfer lens T1 and the acceleration field between T1 and T2. The first transfer lens, T1, shields the dispersive element from the retarding field, while the transfer lens T2 shields the collision cell from the front part of the monochromator, in particular, from the acceleration field. Simion calculations have shown that field penetration through those transfer lenses can be neglected: The influence is ∼2 mV for 10 V of applied potential. The collision cell in itself has not yet been changed (although this will be the next step); only the exit and entrance orifice have been removed. The reason for the removal was that these electrodes were highly magnetic (in the order of the magnitude of the earth's magnetic field) and that their diameter was too small (i.e., 1 mm). This small diameter deteriorated the performance through surface effects and energy-dependent transmission through the small orifices.

The whole lens stack after the collision cell constitutes a retarding field analyzer. This analyzer has

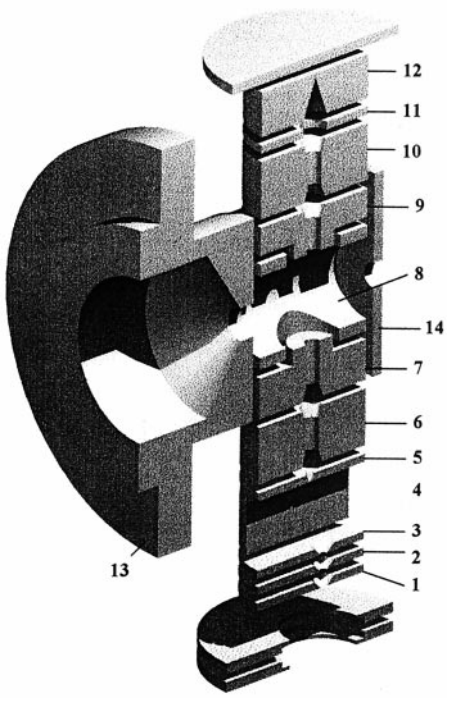

Fig. 12. 3-dimensional scaled view of the newly designed monochromator. The different electrodes are: 1, pusher; 2, entrance electrode 1; 3, entrance electrode 2; 4, dispersive element; 5, exit lens; 6, transfer lens T1; 7, transfer lens T2; 8, collision chamber; 9, transfer lens T3; 10, retarding lens T4; 11, shielding lens; 12, Faraday cup; 13, ion exit lens; 14, neutral beam entrance orifice.

been incorporated into this set-up to have an independent method to determine the energy resolution of the electrons. The first lens, T3, which is symmetric to T2, has the same purpose as T2, namely, to shield the collision cell. After T3, another thick retarding field lens T4 has been added to determine the energy resolution behind the collision chamber. Finally, electrons are collected in a V-shaped Faraday cup directly connected to a floating picoamperemeter. The lens in front of the Faraday cup is necessary for sensitive current measurements to avoid capacitive coupling between T4 and the electron collector. In the case of a correct alignment of the magnetic field, the amount of electrons lost on electrodes before the Faraday cup is rather low. We found that it is advantageous to use such thick lenses for the retarding field analyzer, as otherwise, the retarding field at the center of the lens was not proportional to the applied field and the obtained energy resolution was incorrect. As mentioned previously, this effect is caused by field penetration from adjacent lenses and can be corrected by using either grids instead of the lenses or thick lenses. Although using grids gives similar results as using thick lenses, the transmission through the thick lenses is higher, and therefore, we used this principle.

One important advantage of this new set-up is the possibility to determine the energy resolution at three different points in the monochromator. Moreover, it turns out that the resolutions measured at all three points are rather similar, allowing us to give a reliable number for the resolution that is valid for the whole energy range under consideration. The first point to determine the energy resolution for specific electron energy is immediately after the dispersive element, using T2 as retarding lens and measuring the electron current at the Faraday cup as a function of the voltage applied to T2. In a similar way, but now for a whole set of different electron energies, the energy resolution was determined after the collision cell in the retarding field analyzer, using T4 as a retarding lens. The resolutions determined in this way for different energies are now in fair agreement to the FWHM of the Cl^- curve produced in the collision cell [33]. (It should be mentioned, though, that a detailed analysis of the retarding potential curves for different, and in particular, higher, energies [see Fig. 11] still shows a slight decrease in energy resolution with increasing energy; possible reasons, which are still under investigation, are a misalignment of the magnetic field, stray magnetic fields, and surface effects.) Nevertheless, as can be seen from Fig. 13 under experimental conditions where the Cl^-/CCl_4 curve gives a FWHM of 46 meV, the retarding energy curve measured with the analyzer after the collision cell gives at an electron energy of, for instance, 100 meV a resolution of 45 meV. At present, this is the best resolution we can achieve with this design, but as it is nearly independent of electron energy (see also Fig. 11) and certainly much better than in many other recent applications, we have started to use this apparatus for in-depth investigations of electron attachment to molecules; a first study completed recently has been concerned with several inconsistencies existing in previous

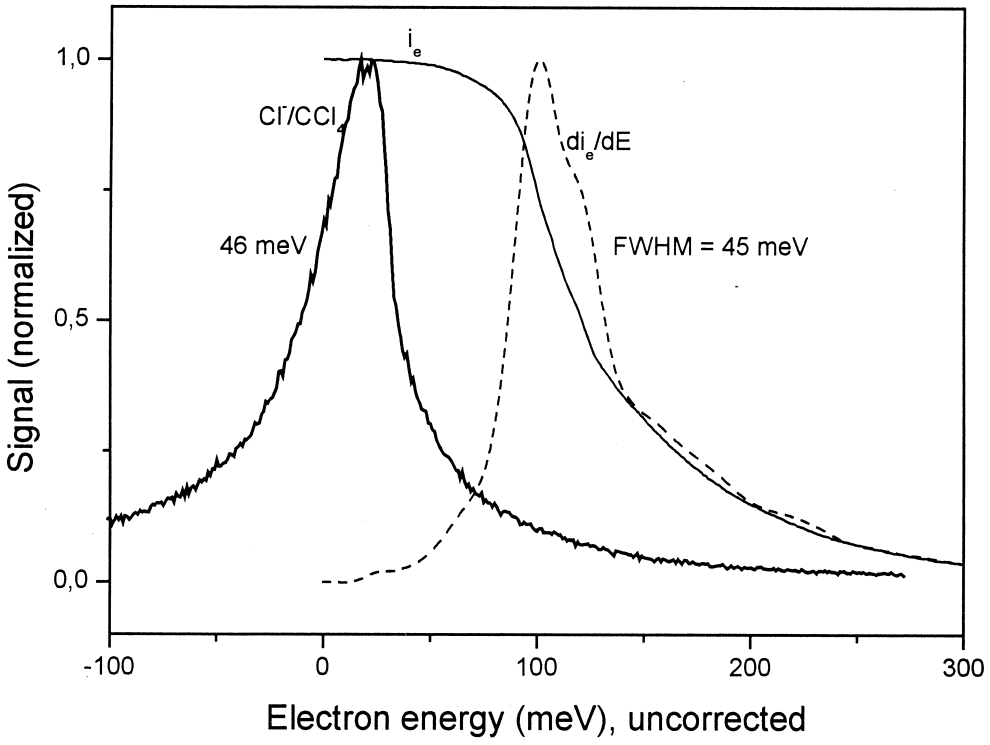

Fig. 13. Comparison of the resolution of the TM (shown in Fig. 12) at about zero eV electron energy as determined by the FWHM of the Cl^- ion current from electron attachment to CCl_4 with the resolution at ~0.1 eV electron energy as determined by measuring the electron current i_e versus retarding voltage and calculating the FWHM of the derivative di_e/dE.

measurements of electron attachment to C_2Cl_4 [34].

Several other slight changes to the monochromator design have been carried out in the course of this study, their main purpose being to allow easier handling of the monochromator. One of these changes, which also improved the signal intensity, was the mounting of the whole monochromator directly onto the ion optics of the quadrupole. This allows a proper adjustment of the monochromator with the center line of the quadrupole, which is quite important, as even a slight misalignment of 0.25 mm will deteriorate the performance of the quadrupole [35]. Another improvement was that we clamped the capillary inlet directly to the neutral beam entrance lens of the collision cell. This enables its fast removal and mounting without need of further alignment.

6. Outlook

As already mentioned in the Introduction, hemispherical monochromators with a resolution of 0.9 meV are available today [1]. This resolution can only be achieved at higher electron energies; nevertheless, it should, in principle, also be possible to improve the performance of trochoidal monochromators to obtain resolutions in this order of magnitude. It is particularly promising that the original trochoidal monochromator [4] and some early follow-ups reported resolutions of ~20 meV [36]. Hence, based on the present results and taking into account the high nominal resolution (in the order of several meV) achieved in our earlier investigations close to zero eV electron energy [7] we are confident that by carefully designing our next generation trochoidal monochromator, this instrument should become a serious competitor to

the hemispherical monochromator in terms of the ultimate resolution achievable. This will allow low-energy electron interaction studies, either in the gas or in the cluster phase, with resolutions so far only achieved in surface analysis. Even appearance energy measurements should be possible with high accuracy.

Acknowledgement

It is a pleasure to be part of the scientific community honoring Alex Stamatovic at his sixtieth birthday. As a frequent visitor to Innsbruck, we have come to know him from day-to-day life in our laboratory as a particularly gifted experimentalist. We are especially indebted for the many stimulating discussions on trochoidal monochromators in the past years, which illustrate his dedicated and lively interest in these devices. Work supported in part by the Fonds zur Förderunp der Wissenschaftlichen Forschung, Vienna, Austria.

References

[1] H. Ibach, D.L. Mills, Electron Energy Loss Spectroscopy and Surface Vibrations, Academic Press, London, 1982.
[2] W.E. Barr, W.A. Perkins, Rev. Sci. Instrum. 37 (1966) 1354.
[3] A. Stamatovic, G.J. Schulz, Rev. Sci. Instrum. 39 (1968) 1752.
[4] A. Stamatovic, G.J. Schulz, Rev. Sci. Instrum. 41 (1970) 423.
[5] D. Roy, Rev. Sci. Instrum. 43 (1972) 535.
[6] M.I. Romanyuk, O.B. Shpenik, Meas. Sci. Technol. 5 (1994) 239.
[7] S. Matejcik, G. Senn, P. Scheier, A. Kiendler, A. Stamatovic, T.D. Märk, J. Chem. Phys. 107 (1997) 8955.
[8] S. Matejcik, A. Kiendler, A. Stamatovic, T.D. Märk, Int. J. Mass Spec. Ion Proc. 149/150 (1995) 311.
[9] H. Hotop, D. Klar, J. Kreil, M.W. Ruf, A. Schramm, J.M. Weber, in L.J. Dube, J.B.A. Mitchell, J.W. McConkey, and C.E. Brion, Eds. The Physics of Electronic and Atomic Collisions, American Institute of Physics, New York, 1995.
[10] A. Chutjian, S.H. Alajajian, Phys. Rev. A 31 (1985) 2885.
[11] M.T. Frey, S.B. Hill, K.A. Smith, F.B. Dunning, I.I. Fabrikant, Phys. Rev. Lett. 75 (1995) 810.
[12] D. Spencer, G.J. Schulz, J. Chem. Phys. 58 (1973) 1800.
[13] S.C. Chu, P.D. Burrow, Chem. Phys. Lett. 172 (1990) 17.
[14] J.W. Bond, M.P. Gough, J. Phys. D 14 (1981) 1153.
[15] C.E. Klots, Chem. Phys. Lett. 38 (1976) 61.
[16] A. Schramm, I.I. Fabrikant, J.M. Weber, E. Leber, M.-W. Ruf, H. Hotop, J. Phys. B 32 (1999) 2153.
[17] A. Stamatovic, G.J. Schulz, Phys. Rev. 188 (1969) 213.
[18] P.J. Chantry, Phys. Rev. 172 (1968) 125.
[19] G. Denifl, D. Muigg, A. Stamatovic, T.D. Märk, Chem. Phys. Lett. 288 (1998) 105.
[20] Y. Chu, G. Senn, P. Scheier, A. Stamatovic, T.D. Märk, F. Brüning, S. Matejcik, E. Illenberger, Phys. Rev. A57 (1998) R697.
[21] M. Allen, J. Electr. Spectroscopy Rel. Phenom. 48 (1989) 219.
[22] D. A. Dahl, SIMION 3D Version 6.0 (1995).
[23] I.D. Williams, R.W. O'Neill, Meas. Sci. Technol. 6 (1995) 1133.
[24] M.R. McMillan, J.H. Moore, Rev. Sci. Instrum. 51 (1980) 944.
[25] S. Matejcik, P. Eichberger, B. Plunger, A. Kiendler, A. Stamatovic, T.D. Märk, Int. J. Mass Spectrom. Ion Proc. 144 (1995) L13.
[26] A. Kiendler, S. Matejcik, J.D. Skalny, A. Stamatovic, T.D. Märk, J. Phys. B 29 (1996) 6217.
[27] S. Matejcik, A. Kiendler, P. Stampfli, A. Stamatovic, T.D. Märk, Phys. Rev. Lett. 77 (1996) 3771; S. Matejcik, P. Stampfli, A. Stamatovic, P. Scheier, T.D. Märk, J. Chem. Phys. 111 (1999) 3548.
[28] J.D. Skalny, S. Matejcik, A. Kiendler, A. Stamatovic, T.D. Märk, Chem. Phys. Lett. 255 (1996) 112; S. Matejcik, P. Cicman, A. Kiendler, J.D. Skalny, E. Illenberger, A. Stamatovic, T.D. Märk, Chem. Phys. Lett. 261 (1996) 437; G. Senn, J.D. Skalny, A. Stamatovic, N.J. Mason, P. Scheier, T.D. Märk, Phys. Rev. Lett. 82 (1999) 5028.
[29] S. Matejcik, P. Cicman, A. Kiendler, G. Senn, E. Illenberger, T.D. Märk, Chem. Phys. Lett. 267 (1997) 329.
[30] Y. Chu, G. Senn, S. Matejcik, P. Scheier, P. Stampfli, A. Stamatovic, E. Illenberger, T.D. Märk, Chem. Phys. Lett. 289 (1998) 521.
[31] V. Grill, H. Drexel, W. Sailer, M. Lezius, T.D. Märk, J. Mass Spectrom., in press (2000).
[32] N. Anderson, P.P. Eggleton, R.G.W. Keesing, Rev. Sci. Instrum. 38 (1967) 924.
[33] To ensure that this Cl^- anion signal used for calibration, measured after mass selection in the quadrupole, is really representative for the production of negative ions in the collision cell, the negative ion signal was also measured at the ion exit lens. This comparison was necessary because, in principle, it would be possible to extract only ions into the quadrupole, which are produced at a particular region in the collision cell. But as the shape of these anion signals measured in both ways as a function of electron energy was similar, the anion signal at the detector is really a representative measure for the anions produced in the collision cell.
[34] W. Sailer, V. Grill, H. Drexel, M. Lezius, T.D. Märk, Physik Event ÖPG 2000, Graz, Austria, Book of Abstracts, p. 86.
[35] P.H. Dawson, ed., Quadrupole Mass Spectrometry and its Applications, AIP Press, Woodbury, NY, 1995.
[36] R. Abouaf, R. Paineau, F. Fiquet-Fayard, J. Phys. B Atom. Molec. Phys. 9 (1976) 303.